

Bottomonium spectroscopy at Belle II

F. TESTA⁽¹⁾⁽²⁾ ON BEHALF OF THE BELLE II ITALIAN COLLABORATION

⁽¹⁾ *Dipartimento di Fisica, Università degli Studi di Torino, via P. Giuria 1, Torino 10125, Italy*

⁽²⁾ *INFN Sezione di Torino, via P. Giuria 1, Torino 10125, Italy*

Summary. — Quarkonium, the bound state of heavy $q\bar{q}$ quarks, is an ideal environment to test QCD at low energy and study the interplay between perturbative and effective theories.

Unexpected exotic states were discovered in the years both in the charmonium and in the bottomonium spectrum, and while new models and interpretations are plenty, the precise nature of such states is yet unclear.

During Run 1, Belle II has recorded a total of 424 fb^{-1} from e^+e^- collision around the $\Upsilon(4S)$ mass region. With this dataset we can explore multiple channels and access a consistent region of the bottomonium spectrum, in order to test our models for the QCD at low energy and better understand the nature of the exotic states. Here we present an overview of some recent Belle II results on bottomonium spectroscopy.

1. – Introduction

Quarkonium is the bound state of charm or bottom quark and their anti-quarks. Due to the large mass of the quarks with respect to their binding energy, the relative velocity β is small, thus allowing to treat their interaction expanding the QCD hamiltonian in terms of β . This create a hierarchy for the processes that happen at the scale of the mass m $\mathcal{O}(1)$, relative momentum p $\mathcal{O}(\beta)$ and kinetic energy E $\mathcal{O}(\beta^2)$ of the quarks and allows one to disentangle the contribution from the different scales, using effective theories such as the potential non relativistic QCD [1] [2] (pNRQCD) or lattice QCD [3] [4] in addition to more straightforward potential models [5]. The spectra of both charmonium and bottomonium, composed by narrow states with well defined quantum number J^{PC} , represent clear environments in which predictions from such effective theories can be tested, in order to advance our understanding of QCD at low energy.

Alongside the so called conventional states, i.e. the ones describable as a $q\bar{q}$ bound state, many exotic candidates have been found in the spectra of both charmonium and bottomonium, starting from the discovery of X(3872) by Belle in 2003 [7]. Since the masses and the properties such isospin, width and decay modes of the exotic bound states cannot be described by a simple $q\bar{q}$ model, additional degrees of freedom in the form of

light quarks or gluons have been introduced, giving birth to a number of effective QCD models, such as molecules, tetraquarks, glueballs or hybrids. However for most of them there is not a clear interpretation yet and distinguishing between models or falsifying one of them is the main challenge of contemporary heavy hadron spectroscopy. One of the most recent addition to the exotic candidates in the bottomonium spectrum was found by Belle in 2019 as an unexpected enhancement in the $\sigma(e^+e^- \rightarrow Y(1, 2, 3S)\pi^+\pi^-)$ [6] at around 10.750 GeV, where no conventional state was expected; this was interpreted as a 1^{--} exotic bound state and named $Y(10753)$ and further evidence was provided by a global analysis of the inclusive and exclusive cross section for $e^+e^- \rightarrow b\bar{b}$ [8].

At the present time Belle II is the only collider experiment working in the region of the bottomonium masses, with 363 fb^{-1} of data collected from e^+e^- collision with \sqrt{s} at the $Y(4S)$ mass region; another 19 fb^{-1} were collected on four energy points around 10.750 GeV during a scan above the $Y(4S)$, in order to measure the cross section of multiple channels to better constraint the hypotheses on the nature of the $Y(10753)$. Here we present an overview of the most recent results from analyses using this dataset.

2. – Observation of the $Y(10753) \rightarrow \omega\chi_{bJ}(1P)$ and search for $X_b \rightarrow \omega\Upsilon(1S)$ at \sqrt{s} near 10.75 GeV

The goal of this analysis[9] was to test the interpretation of the $Y(10753)$ as a mixture of the conventional 4S and 3D states, which predicts comparable branching fractions for $Y(10753) \rightarrow \pi^+\pi^-\Upsilon(1S)$ and $Y(10753) \rightarrow \omega\chi_{bJ}(1P)$ [10] both of the order of 10^{-3} , and a factor of around 0.2 between $\mathcal{B}(Y(10753) \rightarrow \omega\chi_{b1})$ and $\mathcal{B}(Y(10753) \rightarrow \omega\chi_{b2})$ [11]. This analysis also searched for a X_b signal, the bottomonium counterpart of the $X(3872)$, via the $e^+e^- \rightarrow \gamma X_b, X_b \rightarrow \omega\Upsilon(1S)$ channel, which shares the same final state as the $Y(10753) \rightarrow \omega\chi_{bJ}, \chi_{bJ} \rightarrow \gamma\Upsilon(1S)$ decay. The first process is below the kinematic threshold at the first energy point so it was performed using just the data collected at $\sqrt{s} = 10.701, 10.745$ and 10.805 GeV, while the second measurement used the full scan dataset.

2.1. $Y(10753) \rightarrow \omega\chi_{bJ}(1P)$. – Final states $\omega \rightarrow \pi^+\pi^-\pi^0$ and $\chi_{bJ} \rightarrow \gamma\Upsilon(1S)(\rightarrow e^+e^-/\mu^+\mu^-)$ are reconstructed exclusively and the signal is extracted with a two dimensional fit to $M(\gamma\Upsilon(1S))$ versus $M(\pi^+\pi^-\pi^0)$ for the data collected at $\sqrt{s} = 10.745$ and 10.805 GeV, while signal at 10.701 is extracted by counting the events and subtracting the expected background. Distribution of $M(\gamma\Upsilon(1S))$ and $M(\pi^+\pi^-\pi^0)$ is shown in Figure 1, significant signals of χ_{b1} and χ_{b2} is found at 10.745 GeV. Figure 1 shows also the computed Born cross section and the fit function for $e^+e^- \rightarrow \omega\chi_{b1}$ and $e^+e^- \rightarrow \omega\chi_{b2}$, a significant enhancement of the cross section can be observed near 10.745 GeV, consistent with the $Y(10753)$ state. The observed ratio between $\sigma_B(e^+e^- \rightarrow \omega\chi_{b1})$ and $\sigma_B(e^+e^- \rightarrow \omega\chi_{b2})$ was found to be 1.3 ± 0.6 at $\sqrt{s} = 10.745$ GeV, contradicting a pure D wave hypothesis of this state, which would give a value for this ratio around 15[12], and with 1.8σ of difference from the expected value of 0.2 for a 4S-3D mixture.

2.2. $X_b \rightarrow \omega\Upsilon(1S)$. – Search for the X_b in $e^+e^- \rightarrow \gamma X_b$ is conducted reconstructing $X_b \rightarrow \omega\Upsilon(1S)$ at $\sqrt{s} = 10.653, 10.701, 10.745, 10.805$ GeV. Figure 2 reports the distribution of $M(\omega\Upsilon(1S))$ in the expected region of mass for the X_b after the selection, showing reflections from $e^+e^- \rightarrow \omega\chi_{bJ}$, but no evidence of other narrow structures. We set an upper limits at 90% Bayesian credibility for the products of the Born cross section and the branching fraction for $X_b \rightarrow \omega\Upsilon(1S)$ at 0.55, 0.84 and 0.37 pb for the 10.653,

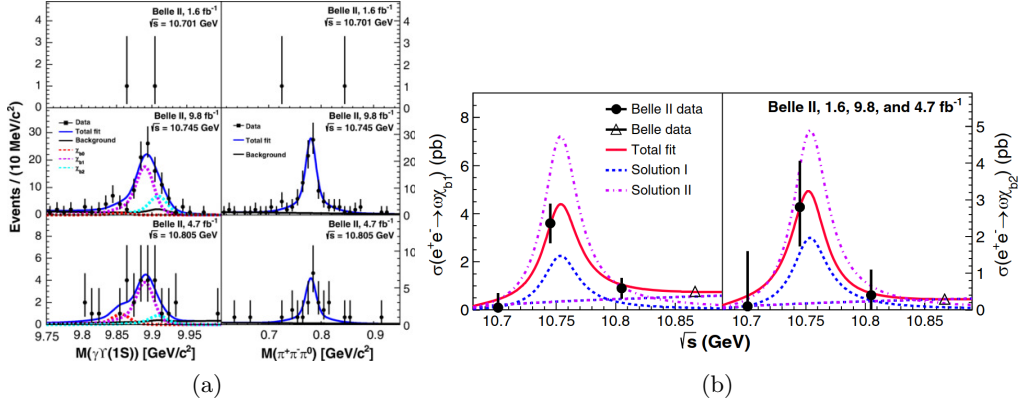


Fig. 1. – Distribution of the reconstructed χ_{bJ} and ω candidates in (a): black points are data and blue line is represent the fit function. Born cross section for the two processes in (b): black dots are the computed values, empty triangle is the Belle result and red line is the fit function.

10.701, 10.745 and 10.805 GeV energies respectively.

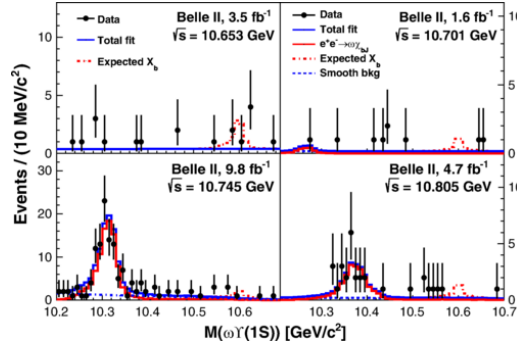


Fig. 2. – Distribution of the mass for the X_b candidates at the four energy points: black points are data and solid line is the fit function, the peaking distribution in the two highest energy point are due to the reflection from $e^+e^- \rightarrow \omega\chi_{bJ}$ signal.

3. – Search for the $e^+e^- \rightarrow \eta_b(1S)\omega$ and $e^+e^- \rightarrow \chi_{b0}\omega$ at $\sqrt{s} = 10.745$ GeV

The search for the $e^+e^- \rightarrow \eta_b(1S)\omega$ is a relevant measurement in our understanding of the $Y(10753)$ since its cross section is predicted to be strongly enhanced with respect to the $e^+e^- \rightarrow \Upsilon(1S)\pi^+\pi^-$ decay in the tetraquark model from Ref [14]. This analysis also searched for the $e^+e^- \rightarrow \chi_{b0}\omega$ with an inclusive approach in order to compare its cross section with the $e^+e^- \rightarrow \chi_{b1/2}\omega$ process, which are predicted to be of the same order in the 4S-3D mixture interpretation of the $Y(10753)$ [11]. For this measurement we used data recorded by Belle II at $\sqrt{s} = 10.745$ GeV, which is the closest to the $Y(10753)$ resonance out of the four points of the scan and the one with larger statistics. In both of the measurements of this analysis [13] the ω candidates are reconstructed in the $\omega \rightarrow \pi^+\pi^-\pi^0$ decay, and the signal is extracted from the recoil mass of the ω defined

as

$$(1) \quad M_{rec}(\pi^+\pi^-\pi^0) = \sqrt{(\sqrt{s} - E_\omega)^2 - p_\omega^2},$$

where E_ω and p_ω are the energy and the momentum of the $\pi^+\pi^-\pi^0$ combination in the center of mass frame. When non specified, all equations in this work are expressed using natural units ($c = 1$).

The distribution of M_{rec} for candidates around the η_b and χ_{b0} is shown in Figure 3.

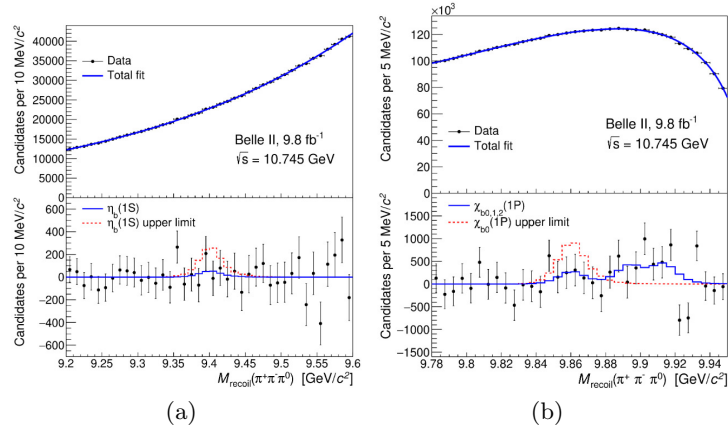


Fig. 3. – Distribution of $M_{rec}(\pi^+\pi^-\pi^0)$ in the η_b (a) and χ_{bJ} mass region. Black dots are data and solid line is the fit function.

No significant excess is found, so we set the following upper limits at 90% CL:

$$(2) \quad \sigma(e^+e^- \rightarrow \eta_b(1S)\omega) < 2.5 \text{ pb}$$

$$(3) \quad \sigma(e^+e^- \rightarrow \chi_{b0}(1P)\omega) < 8.7 \text{ pb}$$

The upper limits on the cross section of χ_{b0} is combined with the result from [9], obtaining

$$(4) \quad \sigma(e^+e^- \rightarrow \chi_{b0}(1P)\omega) < 7.8 \text{ pb}$$

The results do not support the tetraquark interpretation in which the $Y(10753) \rightarrow \eta_b\omega$ process should be enhanced with respect to the $Y(10753) \rightarrow \Upsilon(1, 2, 3S)\pi^+\pi^-$ cross sections, that are in the range of $(1 - 3)\text{pb}$ [6] and it is consistent with the 4S-3D interpretation, in which the $\sigma(\eta_b\omega)$ is expected to be 0.2 – 0.4 times the $\sigma(\Upsilon(nS)\pi^+\pi^-)$ [15].

The upper limit on $e^+e^- \rightarrow \chi_{b0}$ cross section is found greater than the $e^+e^- \rightarrow \chi_{b1}, \chi_{b2}$ cross sections measured in Ref [9], which is consistent with the 4S-3D interpretation that predicts them to be comparable.

4. – Measurement of the energy dependence of the $e^+e^- \rightarrow B\bar{B}, B\bar{B}^*, B^*\bar{B}^*$ cross sections at Belle II

Quarkonium states above the $B\bar{B}$ threshold are expected to decay mostly in $B^{(*)}\bar{B}^{(*)}$ pairs. Belle already measured the cross section of $e^+e^- \rightarrow B\bar{B}, B\bar{B}^*, B^*\bar{B}^*$ [16], but in the range between the $Y(4S)$ and the $Y(6S)$ the fit was poorly constrained by data. This analysis [17] used the data collected by Belle II at 10.653, 10.701, 10.745 and 10.805 GeV to improve the statistics on the aforementioned region. In order to measure the cross sections, one of the B meson is fully reconstructed from a large number of hadronic channels using the multivariate full event interpretation (FEI) algorithm [18]. The signal for the $B\bar{B}, B\bar{B}^*, B^*\bar{B}^*$ process is extracted with a fit on the M_{bc} distribution:

$$(5) \quad M_{bc} = \sqrt{E_{cm}^2/2 - p_B^2},$$

where E_{cm} is the energy of the colliding beams in the center of mass and p_B is the momentum of the reconstructed B meson. Figure 4 shows the distribution of M_{bc} for the four points together with the fit function.

The dressed cross section for each process is computed as

$$(6) \quad \sigma_{dressed} = \frac{N}{(1 - \delta_{ISR})L\epsilon},$$

where N is the signal yield as obtained from the fit on M_{bc} , $(1 - \delta_{ISR})$ is the radiative correction, L is the integrated luminosity and ϵ is the reconstruction efficiency. The results are presented in Figure 4 and are in good agreement with the previous Belle result, while also showing a sharp rise on the $e^+e^- \rightarrow B^*\bar{B}^*$ cross section just above the open flavour threshold, that can hint towards a possible molecular state. This could provide also an explanation for the narrow dip in the $e^+e^- \rightarrow B\bar{B}^*$ cross section as the result of an interference between $e^+e^- \rightarrow B\bar{B}^*$ and $e^+e^- \rightarrow B^*\bar{B}^* \rightarrow B\bar{B}^*$ processes.

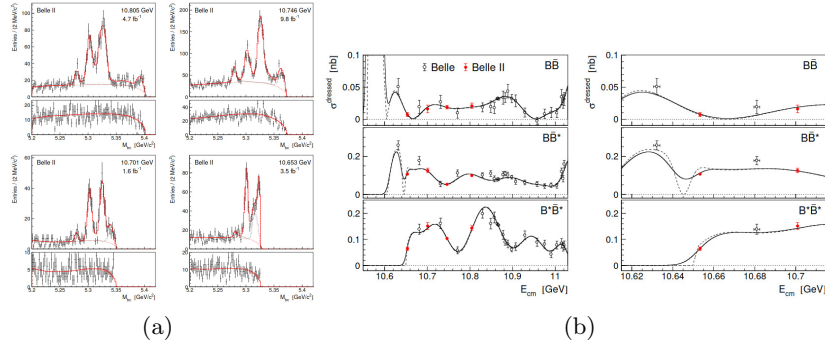


Fig. 4. – Distribution of M_{bc} at the four energies in (a), black dots are data and solid line is the fit function, from left to right the peaking distribution are due to the $B\bar{B}$, $B\bar{B}^*$ and $B^*\bar{B}^*$ contribution. Dressed cross section of the three process in (b), with red dots for the Belle II result, empty dots for previous Belle measurement, solid line for the fit result and dashed line for fit function without accounting for the E_{cm} spread; rightmost image is magnified around the $B^*\bar{B}^*$ threshold.

5. – Conclusion

In this work we presented some recent results from Belle II regarding the interpretation of the $Y(10753)$ state. Results from the measurement of $e^+e^- \rightarrow \chi_{bJ}$ and the $e^+e^- \rightarrow \chi_{b0}$ suggest a 4S-3D interpretation and the upper limits on $e^+e^- \rightarrow \eta_b$ do not support the tetraquark model from Ref [14]. Future measurements of the cross section of other process like $e^+e^- \rightarrow h_b(1P)\pi^+\pi^-$, $e^+e^- \rightarrow \eta h_b(1P)$ and $e^+e^- \rightarrow \eta Y(1D)$ are planned in order to bring more clarity in the study of the $Y(10753)$. We also presented new results on the energy dependence of the cross section of $e^+e^- \rightarrow B\bar{B}, B\bar{B}^*, B^*\bar{B}^*$ around the $Y(10753)$, which are consistent with previous measurements and highlight a sharp rise of the cross section of $e^+e^- \rightarrow B^*\bar{B}^*$ around the kinematic threshold which suggests a molecular state nearby.

REFERENCES

- [1] A.PINEDA and J.SOTO, *Nucl.Phys. B(Proc. Suppl.)*, **64** (1998) 428.
- [2] N. BRAMBILLA, A. PINEDA, J. AOTO and A. VAIRO, *Rev. Mod. Phys.*, **77** (2005) 1423
- [3] G.T.BODWIN, D.K.SINCLAIR and S.KIM, *Phys.Rev.Lett*, **77** (1996) 2376-2379
- [4] T.BURCH *et al.*, *Phys.Rev.D.*, **81** (2010) 034508
- [5] E.EICHEN *et al.*, *Phys.Rev.Lett*, **36** (1976) 1276
- [6] MIZUK R. *et al.*, *Journal of High Energy Physics*, **10** (2019) 220.
- [7] S.-K. CHOI *et al.* (BELLE COLLABORATION), *Phys. Rev. Lett.*, **91** (2003) 262001.
- [8] HÜSKEN, N. AND MITCHELL, R. E. and SWANSON, E. S., *Phys. Rev. D*, **9** (2022) 106.
- [9] ADACHI I. *et al.*, *Phys. Rev. Lett.*, **9** (2023) 130.
- [10] BAI, ZI-YUE and LI, YU-SHUAI and HUANG, QI and LIU, XIANG and MATSUKI, TAKAYUKI, *Phys. Rev. D*, **7** (2022) 105.
- [11] LI, YU-SHUAI and BAI, ZI-YUE and HUANG, QI and LIU, XIANG., *Phys. Rev. D*, **3** (2021) 104;
- [12] FENG-KUN GUO and ULF-G. MEISSNER and CHENG-PING SHEN, *Physics Letters B*, **738** (2014) , pp. 172-177.
- [13] THE BELLE II COLLABORATION, e-Print in <https://doi.org/10.48550/arXiv.2312.13043> [hep-ex].
- [14] ZHI-GANG WANG, *Chinese Physics C*, **43** (2019) 123102.
- [15] S. LIU, Z. CAI, Z. JIA, G. LI and J. XIE, e-Print in <http://arxiv.org/abs/2312.02761> [hep-ph].
- [16] R. MIZUK, *Journal of High Energy Physics*, **6** (2021) 137
- [17] THE BELLE II COLLABORATION, e-Print in <https://arxiv.org/abs/2405.18928v1> [hep-ex]
- [18] T. KECK *et al.*, *Comput. Softw. Big Sci.*, **3** (2019) 6